Jurnal Teknologi

Full Paper

LANDSAT TM-8 DATA FOR RETRIEVING SALINITY IN AL-HUWAIZAH MARSH, SOUTH OF IRAQ

Hashim Ali Hasab[a,b], Anuar Ahmad[a], Maged Marghany[c*], Abdul Razzak Ziboon[d]

[a]Faculty of Geoinformation Science and Real Estate (FGHT), Universiti Teknologi Malaysia, UTM Johor Bahru, Malaysia
[b]Ministry of Higher Education & Scientific Research, Foundation of Technical Education, Baghdad, Iraq
[c]Geoscience and Digital Earth Center (Geo-DEC) Research Institute for Sustainability and Environment
[d]Ministry of Higher Education, University Technology, Construction and Building Dept, Baghdad, Iraq

Article history
Received
19 January 2015
Received in revised form
11 February 2015
Accepted
15 June 2015

*Corresponding author
magedupms@gmail.com

Graphical abstract

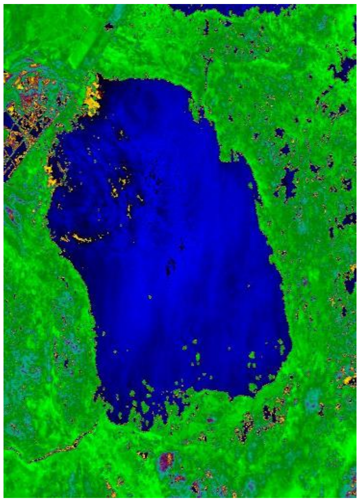

Abstract

Mesopotamia marshlands constitute the largest wetland ecosystem in the Middle East and western Eurasia. These marshlands are located at the confluence of Tigris and Euphrates rivers in southern Iraq. Al-Huwaizah marsh is the biggest marsh in southern Iraq covered by an area (2400 Km^2-3000 Km^2) and depth (1.5 m-5 m). The construction dams by Turkey and Syrian for water storage as well as hydroelectric power generation along Tigris and Euphrates rivers, led to reduce and deteriorate water quality in Iraq's marshes. Salinity has become one of the major problems affecting crop production and food security in central and southern Iraq. The objective of this study to develop a new algorithm to retrieve salinity and normalized difference vegetation index (NDVI) from optical remote sensing Landsat-8 (OLI/TIRS) data based on differential equations algorithms. The mathematical algorithms are linear, power and exponential algorithm. The integration between remote sensing techniques and geographic information system (GIS) to map hydrodynamic and the spatial variation of salinity distribution. There is a pressing need to quantify and map the spatial extent and distribution of the salinity in Al-Huwaizah marsh of southern Iraq during March-2013. The findings of this study proved that the integration between Landsat-8 data and GIS with salinity algorithms could provide a powerful tool for retrieving salinity in marshes zone.

Keywords: Water quality, salinity modeling, remote sensing, NDVI, GIS

Abstrak

Tanah paya Mesopotamia merupakan ekosistem tanah lembap yang terbesar di Timur Tengah dan barat Eurasia. Tanah paya ini terletak di pertemuan Sungai Tigris dan Euphrates di selatan Iraq. Paya Al-Huwaizah adalah salah satu paya Iraq yang terbesar di selatan Iraq yang dilitupi oleh kawasan (2400 Km^2-3000 Km^2) dan kedalaman (1.5 m-5 m). Pembinaan empangan oleh Turki dan Syria untuk simpanan air serta penjanaan kuasa hidroelektrik di sepanjang Sungai Tigris dan Euphrates telah mengakibatkan pengurangan dan kemerosotan kualiti air dalam paya Iraq. Kemasinan telah menjadi salah satu masalah utama yang memberi kesan kepada pengeluaran tanaman dan keselamatan makanan di tengah dan selatan Iraq. Objektif kajian ini untuk membangunkan algoritma baru untuk mendapatkan semula kemasinan dan indeks tumbuhan perbezaan normal (NDVI) daripada data optikal penderiaan jauh Landsat-8 (OLI/TIRS) berdasarkan perbezaan persamaan algoritma. Algoritma matematik adalah linear, kuasa dan algoritma eksponen. Integrasi diantara teknik penderiaan jauh dan sistem maklumat geografi (GIS) adalah untuk pemetaan hidrodinamik dan perubahan spatial taburan kemasinan. Terdapat keperluan mendesak untuk mengukur dan pemetaan liputan spatial dan taburan kemasinan dalam paya Al-Huwaizah di selatan Iraq pada bulan Mac 2013. Hasil kajian ini membuktikan bahawa integrasi di antara data Landsat-8 dan GIS dengan menggunakan algoritma kemasinan boleh digunakan sebagai alat yang berkuasa untuk mendapatkan semula kemasinan di zon paya.

Kata kunci: Kualiti Air, permodelan kemasinan, penderiaan jauh, NDVI, GIS

1.0 INTRODUCTION

In the last century, there are several critical environmental problems have been raised up such as environmental pollution [1, 2] poor water quality supply sanitation and soil erosions [3]. Man-made is beyond all the environmental crises due to destructive wars. It is not forgotten the three decades of the Gulf wars of 1980, 1991 and 2003, respectively, which led to several damages of the environment, especially in Arabian Gulf coastal waters and in Iraq. For instance, during the1991Gulf War, roughly one million oil tones blackened the Arabian Gulf. Further, the three decades of war have destroyed Iraq's water resources management system. Thus, Iraq confronts complications to recognize the target of 91% of households using safe drinking water supply by 2015. Presently, 16% of households convey daily difficulties with supply and 20% use as an unsafe drinking water source. Furthermore, leaking sewage pipes and septic tanks pollute the drinking water network [4, 5, 6, 7].

In Iraq, there are other problems have risen up in last decades, such as water quality. American-Iraq war in 2003 has been affecting the water quality of rivers, streams, lakes and marshes in Iraq [3, 8]. Further, inadequately treated sewage, poor land use practices, industrial waste waters discharges excessive use of fertilizers, and a lack of integrated watershed management are other factors impact water quality in Iraq [3]. The effects of these problems threaten ecosystems, endanger public health risks, and intensify erosion and sedimentation, leading to land and water resources degradation. Many of these negative effects arise from environmentally destructive development, a lack of information on the situation regarding water quality and poor public awareness and education on the protection of water resources [3, 8, 9].

However, clean water is essential to human survival as well as to aquatic life. Much surface water is used for irrigation, with lesser amounts for municipal, industrial, and recreational purposes only 6% of all inland water is used for domestic consumption. An estimated 75% of the population of developing nations lacks adequate sanitary facilities and solid waste is commonly dumped into the nearest body of flowing water. Pathogens such as bacteria, viruses and parasites make these waste materials among the world's most dangerous environmental pollutants, waterborne diseases are estimated to cause about 25,000 deaths daily worldwide [9, 10, 11, 12].

Predicted bivariate and multiple regression (MR) techniques based on Landsat-5TM multispectral to investigate spatial patterns for water quality parameters such as Suspended sediment (SS), turbidity, Secchi disk depth (SDD), and chlorophyll-a (chl-a) in Lake Beysehir, which is the largest freshwater reservoir in Turkey. The combinations of TM bands, band ratios and single TM bands estimated and correlated with the measured water quality parameters. The best regression models were ($0.60 < R^2 < 0.71$). TM3 provided a significant relationship with Suspended sediment concentration is (R^2=0.67, p<0.0001). Multiple regression (MR) between the various combinations of TM bands and chlorophyll-a, is (R^2=0.60, p<0.0001) that showed TM1, TM2, and TM4 are strongly correlated with measured chl-a concentrations. MR showed that TM1, TM2, and TM3 explain 60% (p< 0.0001) of the variance in turbidity, while MR with R^2=0.71 (p<0.0001) showed that TM1/TM3 and TM1 band combinations was a strong relationship with measured SDD [13].

Developed a neural network model and used optical sensors such as Landsat TM to monitor and quantify a water quality parameters such as phosphorus, chl-a and turbidity in the Kissimmee river basin in south Florida before and after ecosystem restoration and during the dry and wet seasons. They explored there are excellent relationship between the simulated and observed water quality parameters depending on the development of neural network model. They found in 1998–1999 and in 2009–2010 during dry and wet seasons the correlated for a specific region in the greater Florida Everglades is R^2>0.95 and the value of the root mean square error for phosphorus is below 0.03 mg L^{-1} and for turbidity is 0.5 NTU then for a chlorophyll-a is 0.17 mg m^{-3}. Used the development methodology investigated for spatial and temporal dynamics of the selected water quality parameters [14].

Used remote sensing to detect one of the water quality parameters such as total phosphorus (TP) concentrations depending on the use of support vector regression (SVR) machine and a new TP remote sensing algorithm for optically complex turbid inland waters in Lakes Taihu, Chaohu, Dianchi, and Three Gorges reservoir of China at specific times during 2009~2011.

Normalized trough depth of spectral reflectance at 675 nm (NTD675) for first classified of water classification methods, Then used several band ratios from spectral regions sensitive specifically to explore and express for each water type. Used spectral ranging for three types such as for T1: a710/691, 706/691, 714/691 and T2: 769/629, 769/625, 769/633 then T3: 765/551, 765/556, 765/559. They explored SVR algorithms yield relatively high predictive accuracies. The mean absolute percentage errors for T1, T2, and T3 waters produced with the independent validation samples achieved at 32.7, 23.2, and 14.1 %, respectively. SVM algorithm has been high accuracy more than an aggregated SVR algorithm. It applications with HJ1A/HSI image data that demonstrates the algorithms have a good potential for estimating TP concentrations in optically complex turbid inland waters from remote sensing [15].

Remote sensing techniques play major roles for monitoring and mapping, water quality [9, 10]. With advances, using remote sensing for data acquisition and the integrating finite element numerical model with the spatial capabilities of GIS and the spatial and temporal capabilities of remote sensing applications could provide a powerful tool for management and assessment to water quality problems in the marsh zone of southern Iraq [6, 16].

The gap of this paper to develop linear, power and exponential algorithms to retrieve salinity from Landsat-8 (OLI/TIRS) data and integration between remote sensing (RS) with geographic information system (GIS) for assessing and mapping the spatial variation of salinity in Al-Huwaizah marsh south of Iraq during March in 2013.

2.0 MATERIALS AND METHODS

2.1 Study Area

The marshes zone is located south of Iraq between latitudes (32˚00′-32˚30′) N and longitudes (46˚00′-48˚00′) E of the Greenwich meridian. It is representing one of the largest wetland ecosystems in all of Asia and covered more than 19,000 Km^2 and is formed by the confluence of the Tigris and Euphrates rivers. Al-Huweizah marsh is one of the major marsh from marshes southern Iraq, is located east of Tigris River by approximate area (2400Km^2-3000Km^2) and water level (1.5-5) meter (Figure 1). The climate is moderate with 37.7° Celsius mean yearly temperature, (400-1000) millimeter sum of yearly rain, and 49 percent mean relative humidity. This area in 2003 had been reduced in size to less than 7% of their 1973 levels 8,926 Km^2 within Iraq. It considered as a settlement area for birds and fishes, therefore it represents an important source for fishing and agricultural areas [2].

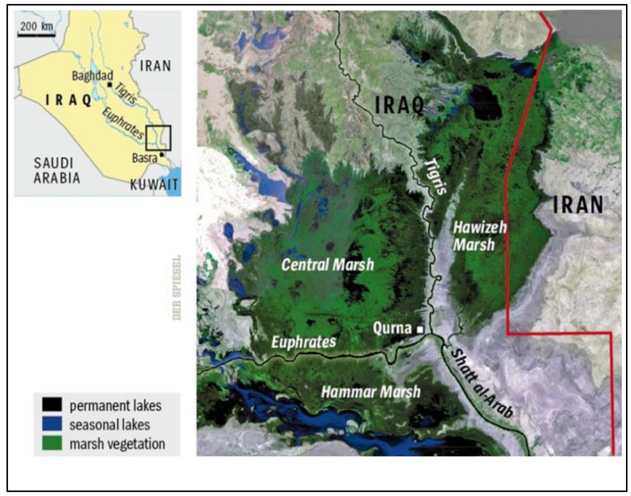

Figure 1 Marshlands south of Iraq

2.2 Methodology

Landsat TM-8 data by path 166 and row 38 used for retrieving salinity in Al-Huwaizah marsh during March in 2013. The spectral signature reflectance cover of water has the characteristic as a general reduction in reflectance with increasing wavelength in the visible wavebands as well as in the near infrared (NIR) such as bands from (B1-B5) are an important bands for water quality parameters and normalized difference vegetation index (NDVI). Develop algorithms such as linear, power and exponential to retrieve water quality parameters such as salinity and (NDVI) from Landsat-8 (OLI/TIRS) data. This selected to identify the normalized difference vegetation index (NDVI) and salinity. The integration between remote sensing data, GIS and mathematical algorithm to determine salinity concentrations and distributions in AL-Huwaizah marsh zone southern Iraq.

2.3 Normalized Difference Vegetation Index (NDVI)

NDVI used in this study to know the vegetations values. NDVI is the ratio between measured reflectance in the red (R) and near infrared (NIR) spectral bands of the images from Landsat-8 (OLI/TIRS) data, It is calculated using the following formula [17, 18].

$$\text{NDVI Landsat} = (\text{Band5}-\text{Band4}) / (\text{Band5}+\text{Band4}) \quad (1)$$

2.4 Data Collection and Model

Data collections are required, such as a hydrological data inflow and outflow of all marshes and topographical data as the marsh boundaries, area, surface water elevation, depth water, geographical location of sources, pollution stations, geographical location for twenty sampling stations as (HZ1-HZ20) and ground data for salinity as well as the satellite images such as Landsat-8 that resolution 30 m^2 with eleven bands. Develop mathematical algorithm such as linear, power and exponential for assessing and monitoring water quality such as salinity and NDVI when integrate with remote sensing techniques and GIS. Salinity algorithm is using the following formula.

Linear Salinity Algorithm= 17159*(NDVI) - 42.57 ± SE (2)
Power Salinity Algorithm= 7578.7*(NDVI) $^{0.672}$ ± SE (3)
Exponential Salinity Algorithm= 507.7*(e) $^{10.176*(NDVI)}$ ± (4)

Standard Error in the salinity (SE) = $\sqrt{\frac{\sum_{i=0}^{n}(y-\bar{y})^2}{n-2}}$ (5)

y : Ground Data
$\bar{y}$: Model data
n : Numbers of Stations.
There are twenty stations numbered as (HZ1-HZ20).

These algorithms are created from the relationship between ground data of salinity and NDVI from Landsat data by using SPSS-22 software then applied by using ENVI and ERDAS software, 2013.

3.0 RESULTS AND DISCUSSION

In order to fulfill the overall aim and objectives of the study, the results and analyses will achieve based on the pre-processing and processing of the input datasets such as Landsat-8 data on March 2013. The obtaining results for (NDVI) depending on optical remote sensing data as shown in the map, profile and values for NDVI in (Figure 2A&2B). Use algorithms for retrieving salinity depending on NDVI values from Landsat data. The correlation coefficient (R^2) between salinity and NDVI in linear is (0.7343), in power is (0.6975) and in exponential is (0.8524) as shown in (Figure 3). The standard error (SE) in linear is (94.33 mg/l), in power is (71.56 mg/l) and in exponential is (51.25 mg/l) as shown (Figure 4). The minimum and maximum of the salinity concentrations values are (402 mg/l) and (3800 mg/l) respectively as shown in (Figure 5). The salinity concentrations values are depending on the geographical location of sampling stations in Al- Huwaizah marsh southren Iraq during March in 2013, as shown in (Figure 6A&6B).

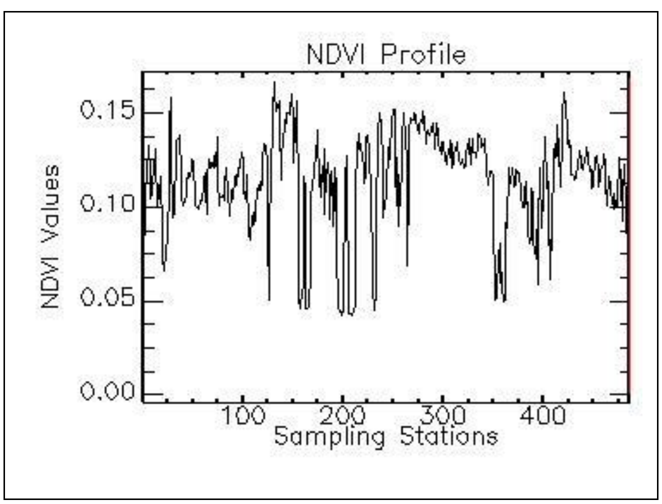

Figure 2-A NDVI profile for Al-Huwaizah marsh in March 2013

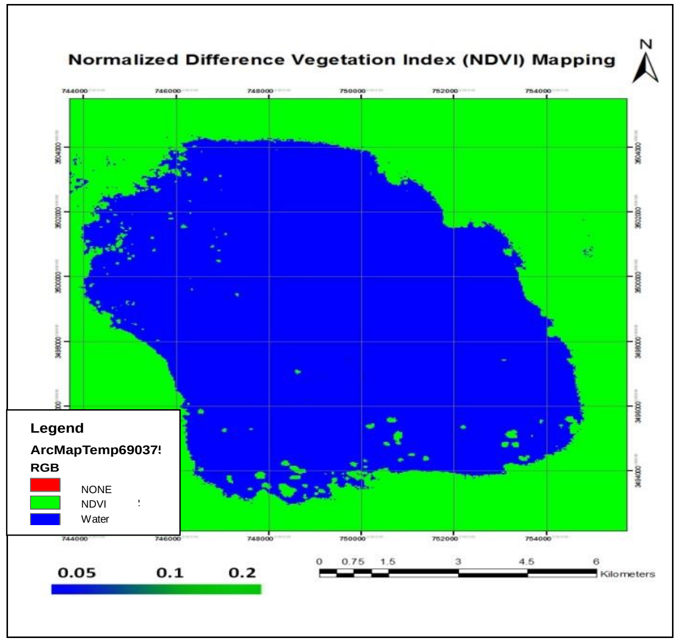

Figure 2-B Normalized difference vegetation index (NDVI) map for Al-Huwaizah marsh in March 2013

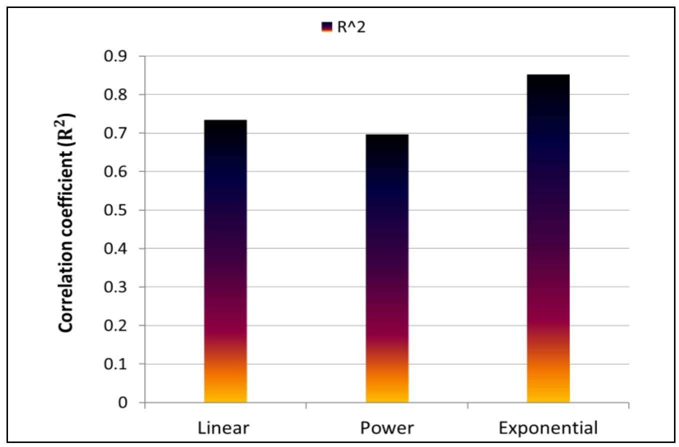

Figure 3 Correlation coefficient values (R^2) for salinity in Al-Huwaizah marsh by using linear, power and exponential algorithms in March-2013

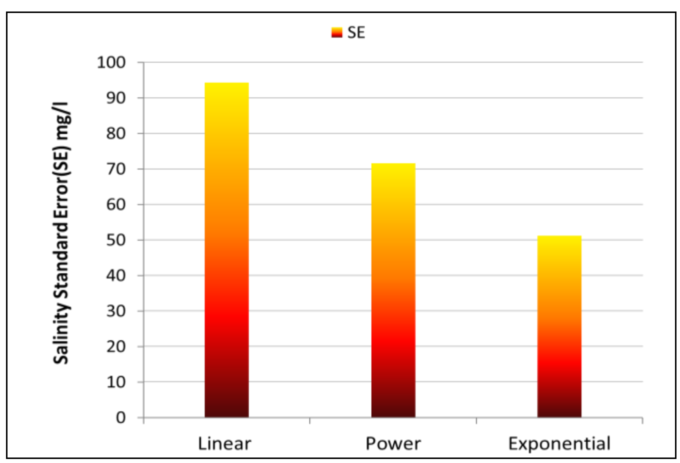

Figure 4 Standard error values (SE) for salinity in Al-Huwaizah marsh by using linear, power and exponential algorithms in March-2013

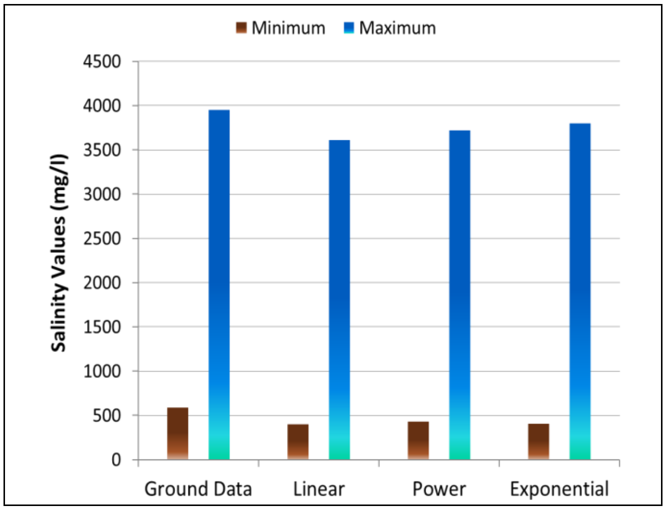

Figure 5 Minimum and maximum of salinity values in ground, linear, power and exponential in Al-Huwaizah marsh by using linear, power and exponential algorithms in March-2013

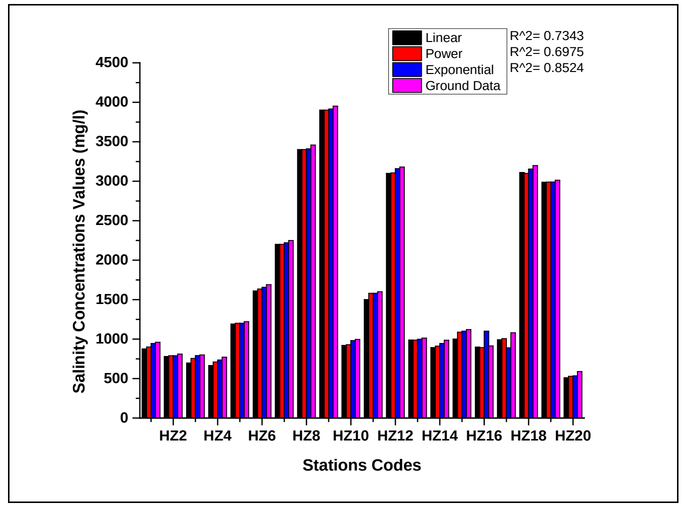

Figure 6-A Salinity concentrations values in Al-Huwaizah marsh depending on ground, linear, power and exponential algorithms in March-2013

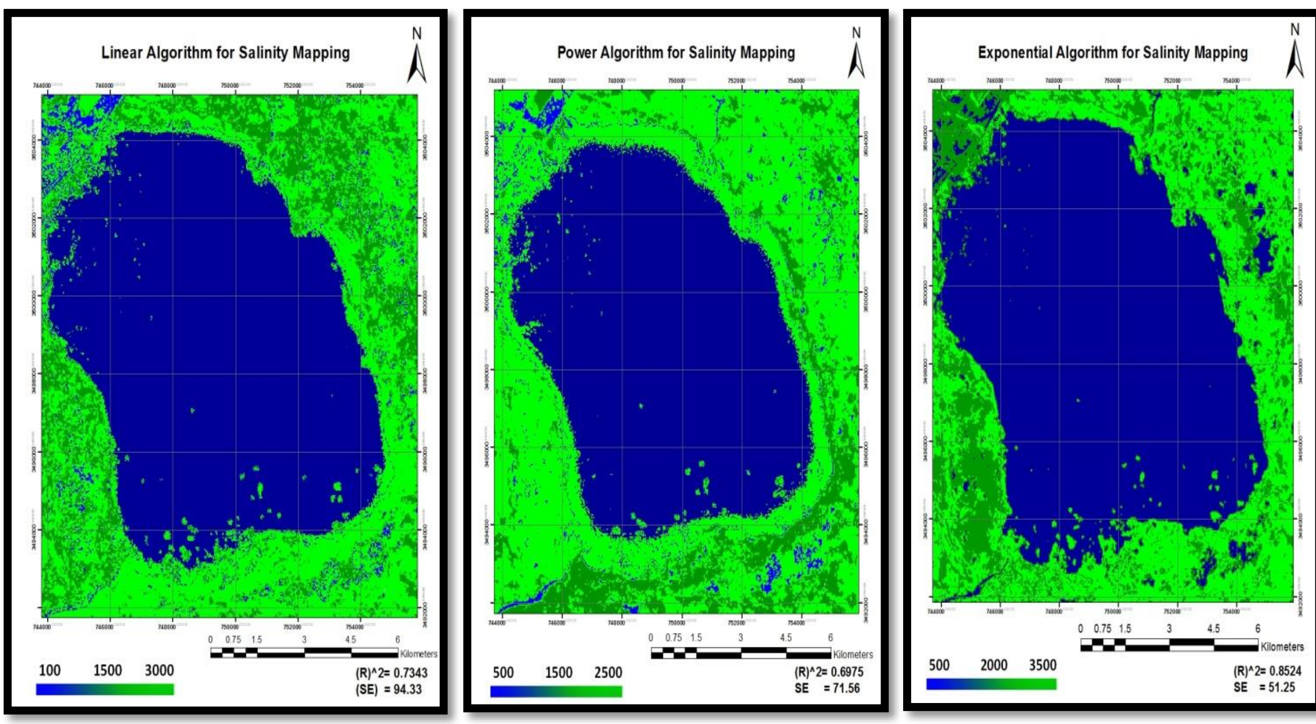

Figure 6-B Salinity maps in Al-Huwaizah marsh by using linear, power and exponential algorithm in March-2013

4.0 CONCLUSION

Optical remote sensing data such as Landsat-8 provide good information about salinity in marsh zone. The integration between Landsat-8 data and GIS with salinity algorithms could provide a powerful tool for retrieving salinity in marshes zone. The salinity algorithms are linear, power and exponential. This study shows the salinity increase in the station HZ9 and decrease in the stations HZ20. The minimum of salinity concentration value is (402 mg/l) and maximum is (38001 mg/l).The standard error (SE) and the correlation coefficients (R^2) in exponential algorithm are (51.25) and (0.8524) respectively. The significance of this study to assess the salinity from Landsat data depending on exponential model. The exponential model has more accurate than linear and power model. That mean the exponential model can be performed high accuracy for salinity when compare with other models. This can prove that there are exponentially relationships between the geographical location of sampling and salinity concentrations in marsh zone.

Acknowledgement

The authors are thankful to Universiti Teknologi Malaysia (UTM), Ministry of Higher Education and Foundation of Technical Education in Iraq for providing the necessary data and facilities for the preparation of the paper. The authors also gratefully acknowledge to Journal Teknology (JT) staff to improve and publish this paper in Scopus indexed.

References

[1] John, P. K., John R. S. and Chester, F.2007. *Hyperspectral Imaging Systems.* 2007. Carlson Center for Imaging Science, Rochester Institute of Technology, Rochester, NY. 19-40.

[2] Abdul Jabbar, M. F., Al-Ma'amar A. F. and Shehab, A. T.. 2010. Change Detections in Marsh Areas, South Iraq, Using Remote Sensing and Gis Applications, Information Department/ Remote Sensing Division in the State Company of Geological Survey and Mining, Iraq. *Iraqi Bulletin of Geology and Mining*. 6(2): 17-39.

[3] Curtiss O. D. and Gia M. L. 2004. *Remote Sensing for Natural Resource Management and Environmental Monitoring*. Naval Research Laboratory Washington, Ch8, (*Costal Margins and Estuaries*). 418-425.

[4] Lowi, M. R. 1995. Rivers of Conflict, Rivers of Peace. *Journal of International Aflairs; Summer* 49: 1.

[5] Lowi, M. R. 1995. Rivers of Conflict, Rivers of Peace. *Journal of International Aflairs; Summer*. 49: 1.

[6] Ammenberg, P., P. Flink, T. Lindell, D. Pierson, and N. Strombeck. 2002. Bio-optical Modelling Combined with Remote Sensing to Assess Water Quality. *International Journal of Remote Sensing*. 23(8): 1621-1638.

[7] Saad, M. and Gaber, A. 2013. Remote Sensing Application for Water Quality Assessment in Lake Timsah, Suez Canal, Egypt. *Journal of Remote Sensing Technology.* 1(3): 61-74.

[8] Bunker, A. L. 2004. Protection of the Environment During Armed Conflict: One Gulf, Two Wars. *Review of European Community & International Environmental Law*. 13(2): 201-213.

[9] Kerekes, J. P. and Baum, J. E. 2005. Full-spectrum Spectral Imaging System Analytical Model. *Geoscience and Remote Sensing, IEEE Transactions*. 43(3): 571-580.

[10] Susan, L. U. 2004. *Remote Sensing for Natural Resource Management and Environmental Monitoring*. 2004. University of California, Davis. 345-400.

[11] Zacharias, I. and Gianni, A. 2008. Hydrodynamic and Dispersion Modeling as a Tool for Restoration Of Coastal Ecosystems. Application to a Re-Flooded Lagoon. *Environmental modelling and Software*. 23: 751-767.

[12] Paul M. M. and Magaly, K. 2011. *Computer Aprocessing of Remotely-sensed Images an Introduction*. Center for Remote Sensing, Boston University. 23-27.

[13] Nas, B., Ekercin, S., Karabörk, H., Berktay, A., & Mulla, D. J. 2010. An Application of Landsat-5TM Image Data for Water Quality Mapping in Lake Beysehir, Turkey. *Water, Air, & Soil Pollution*. 212(1-4): 183-197.

[14] Chebud, Y., Naja, G. M., Rivero, R. G., & Melesse, A. M. 2012. Water Quality Monitoring Using Remote Sensing and an Artificial Neural Network. *Water, Air, & Soil Pollution*. 223(8): 4875-4887.

[15] Sun, D., Qiu, Z., Li, Y., Shi, K., & Gong, S. 2014. Detection of Total Phosphorus Concentrations of Turbid Inland Waters Using a Remote Sensing Method. *Water, Air, & Soil Pollution*. 225(5): 1-17.

[16] Azab, A. M. 2012. *Integrating GIS, Remote Sensing, and Mathematical Modelling for Surface Water Quality Management in Irrigated Watersheds*. Delft, the Netherland. 25-130.

[17] Hazin, S. and Hashim, M. 2014. Separation of Different Vegetation Types in ASTER and Landsat Satellite Images Using Satellite-derived Vegetation Indices. *Jurnal Teknologi (Sciences & Engineering)* 71(4): 109-114.

[18] De Bie, C. J. M., Khan, M. R., Smakhtin, V. U., Venus, V., Weir, M. J. C. & Smaling, E. M. A. 2011. Analysis of Multi-Temporal SPOT NDVI Images for Small-Scale Land-Use Mapping. *International Journal of Remote Sensing*. 32: 6673-6693.

[19] Bandaru, V., West, T. O., Ricciuto D. M. & César I. R.. 2013. Estimating Crop Net Primary Production Using National Inventory Data and MODIS-Derived Parameters. *ISPRS Journal of Photogrammetry and Remote Sensing*. 80: 61-71.

[20] Golafshani, M. B., Shahnazari, A., Ahmadi, M. Z. & Aghajani, G. 2012. Compare the Parameters of the Water Balance In Traditional and Land Levening Paddy Fields in Qaemshahr City. *Journal of Soil and Water*. 1010-1017.

[21] Huang, S., Liu, H., Dahal, D., Jin, S., Welp, L. R., Liu, J. & Liu, S. 2013. Modeling Spatially Explicit Fire Impact on Gross Primary Production in Interior Alaska Using Satellite Images Coupled With Eddy Covariance. *Remote Sensing of Environment.* 135: 178-188.

[22] Jiang, Z., Huete, A. R., Didan, K. & Miura, T. 2008. Development of a Two-band Enhanced Vegetation Index Without a Blue Band. *Remote Sensing of Environment.* 112: 3833-3845.

[23] Kolios, S. & Stylios, C. D. 2013. Identification of Land Cover/Land Use Changes in the Greater Area of the Preveza Peninsula in Greece Using Landsat Satellite Data. *Applied Geography*. 40: 150-160.

[24] Mohamed, M. & Plante, R. 2002. Remote Sensing and Geographic Information Systems (GIS) for Developing Countries. In: *Geoscience and Remote Sensing Symposium*. IGARSS'02. 2002 IEEE International. 2002. IEEE. 2285-2287.

[25] Ninomiya, Y. 2003. A Stabilized Vegetation Index and Several Mineralogic Indices Defined for ASTER VNIR And SWIR Data. *In: Geoscience and Remote Sensing Symposium*. 2003. IGARSS'03. Proceedings. 2003 IEEE International. 1552-1554.

[26] O'connell, J., Connolly, J., Vermote, E. F. & Holden, N. M. 2013. Radiometric Normalization for Change Detection in Peatlands: A Modified Temporal Invariant Cluster Approach. *International Journal of Remote Sensing*. 34: 2905-2924.

[27] Pournamdari, M. & Hashim, M. 2013. Detection of Chromite Bearing Mineralized Zones in Abdasht Ophiolite Complex Using ASTER And ETM+ Remote Sensing Data. *Arabian Journal of Geosciences*. 1-11.

[28] Pu, R. 2012. Mapping Leaf Area Index Over a Mixed Natural Forest Area in the Flooding Season Using Ground-Based Measurements and Landsat TM Imagery. *International Journal of Remote Sensing*. 33: 6600-6622.

[29] Sharma, R., Ghosh, A. & Joshi, P. 2013. Analysing Spatio-Temporal Footprints of Urbanization on Environment of Surat City Using Satellite-Derived Bio-Physical Parameters. *Geocarto International*. 28: 420-438.

[30] Stevens, F. R. 2009. Bridging the Landsat Data Gap: Evaluating ASTER as an Alternative. University of Florida.

[31] Van Den Bergh, F., Wessels, K. J., Miteff, S., Van Zyl, T. L., Gazendam, A. D. & Bachoo, A. K. 2012. HiTempo: A Platform For Time-Series Analysis of Remote-Sensing Satellite Data in a High-Performance Computing Environment. *International Journal of Remote Sensing*. 33: 4720-4740.

[32] Sun, D., Qiu, Z., Li, Y., Shi, K., & Gong, S. 2014. Detection of Total Phosphorus Concentrations of Turbid Inland Waters Using a Remote Sensing Method. *Water, Air, & Soil Pollution*. 225(5): 1-17.